Nodal mutant eXtraembryonic ENdoderm (XEN) stem cells upregulate markers for the anterior visceral endoderm and impact the timing of cardiac differentiation in mouse embryoid bodies

Wenrui Liu[1], Kemar Brown[1], Stephanie Legros[1] and Ann C. Foley[1],*

[1]Greenberg Division of Cardiology, Weill Cornell Medical College, New York, NY 10065, USA

*Author for correspondence (acf2002@med.cornell.edu)

Summary

Interactions between the endoderm and mesoderm that mediate myocardial induction are difficult to study in vivo because of the small size of mammalian embryos at relevant stages. However, we and others have demonstrated that signals from endodermal cell lines can influence myocardial differentiation from both mouse and human embryoid bodies (EBs), and because of this, assays that utilize embryonic stem (ES) cells and endodermal cell lines provide excellent in vitro models to study early cardiac differentiation. Extraembryonic endoderm (XEN) stem cells have a particular advantage over other heart-inducing cell lines in that they can easily be derived from both wild type and mutant mouse blastocysts. Here we describe the first isolation of a *Nodal* mutant XEN stem cell line. *Nodal*$^{-/-}$ XEN cell lines were not isolated at expected Mendelian ratios, and those that were successfully established, showed an increase in markers for the anterior visceral endoderm (AVE). Since AVE represents the heart-inducing endoderm in the mouse, cardiac differentiation was compared in EBs treated with conditioned medium (CM) collected from wild type or *Nodal*$^{-/-}$ XEN cells. EBs treated with CM from *Nodal*$^{-/-}$ cells began beating earlier and showed early activation of myocardial genes, but this early cardiac differentiation did not cause an overall increase in cardiomyocyte yield. By comparison, CM from wild type XEN cells both delayed cardiac differentiation and caused a concomitant increase in overall cardiomyocyte formation. Detailed marker analysis suggested that early activation of cardiac differentiation by *Nodal*$^{-/-}$ XEN CM caused premature differentiation and subsequent depletion of cardiac progenitors.

Introduction

Inductive interactions between endoderm and mesoderm mediate the initial phases of cardiac differentiation in all vertebrates by activating expression of early cardiac markers such as *Nkx2.5* and *Tbx5* (Jacobson, 1960; Orts-Llorca and Gil, 1965; Fullilove, 1970; Sugi and Lough, 1994; Tonegawa et al., 1996; Arai et al., 1997; Schneider and Mercola, 1999; Lough and Sugi, 2000; David and Rosa, 2001; Marvin et al., 2001; Mummery et al., 2003; Yuasa et al., 2005; Brown et al., 2010a; Holtzinger et al., 2010). However, because of the small size and relative inaccessibility of mammalian embryos at pertinent developmental stages, little headway has been made in identifying specific cardiogenic signals in the endoderm. A major advance came with the discovery that visceral endoderm (VE)-like cell lines, such as the embryonal carcinoma-derived END2 cells, can activate and/or increase cardiac differentiation from both mouse and human embryonic stem (ES) cells (Mummery et al., 2003). However, since END2 cells cannot be re-derived from mutant embryos, they cannot be used to study specific inducing factors in the endoderm. We recently showed that XEN cells express markers for the AVE (Brown et al., 2010b) and possess cardiogenic potential similar to END2 cells (Brown

et al., 2010a). XEN cells can easily be isolated from both wild type and mutant mouse embryos. To accomplish this, 3.5 dpc blastocysts are grown in vitro for several days until they attach to feeder cells. At this point, outgrowths of trophoblast cells can be dissected away and the remaining cells dissociated and replated. Ultimately, cell morphology and marker analysis (Brown et al., 2010b) can be used to distinguish primitive endoderm stem cells (XEN cells) from embryonic stem cells (ES cells). We previously demonstrated that XEN cells comprise a heterogeneous population of cells expressing markers for all primitive endoderm derivatives including the parietal endoderm (PE), visceral endoderm (VE) and anterior visceral endoderm (AVE) (Brown et al., 2010b). More recently it has been demonstrated that XEN cells can be directed toward specific endodermal lineages by the addition of growth factors, with BMP directing them to the VE lineage (Artus et al., 2011), and with NODAL directing cells to the AVE lineage (Julio et al., 2011). Because of this, and because primitive endoderm and epiblast remain in contact for at least two days during XEN cell isolation, we hypothesized that signals present in either the epiblast cells or within the primitive endoderm of the isolated blastocyst could influence the specific subtypes of cells that develop in any

given XEN cell line. At preimplantation stages in the mouse, *Nodal* is expressed throughout the epiblast, and both a *Nodal* transgene (Varlet et al., 1997; Brennan et al., 2001; Camus et al., 2006; Mesnard et al., 2006; Granier et al., 2011) and *Nodal* mRNA (Norris et al., 2002; Yamamoto et al., 2004) are transiently expressed in the VE. Moreover, NODAL has been shown to affect AVE marker expression in embryos (Brennan et al., 2001) and in XEN cells (Julio et al., 2011). Therefore, loss of *Nodal* should also impact the specific lineages that become established in XEN cell lines.

To test this, $Nodal^{-/-}$ XEN cells were isolated and characterized by immunocytochemistry, Western blot and QRT-PCR for expression of primitive endoderm (PrE), VE and AVE markers. XEN cells isolated from *Nodal* mutant blastocysts showed a surprising upregulation of AVE markers. EBs that were treated with $Nodal^{-/-}$ XEN CM began to beat earlier than those treated with $Nodal^{+/+}$ XEN CM, suggesting that factors regulated by *Nodal* play a role in regulating temporal aspects of heart development. Finally, we demonstrate that this early activation of cardiac differentiation correlated with an early activation of *Islet-1* expression, which in the embryo, marks cardiac progenitors in the second heart field (SHF). By comparison, expression of *Tbx5* and *Nkx2.5*, markers for the first heart field (FHF), were either unchanged or slightly delayed.

Results

Nodal mutant XEN cell lines were not derived at expected Mendelian ratios

To test the hypothesis that *Nodal* expression in the blastocyst stage embryo impacts the patterning of XEN cells that are isolated from them, XEN cell lines were established from *Nodal* mutant embryos. Because $Nodal^{-/-}$ embryos are not viable, XEN cell lines were established by crossing mice that possessed a heterozygous deletion of *Nodal* ($Nodal^{+/-}$). Blastocysts of unknown genotype were isolated at 3.5 dpc, and XEN cell lines were derived according to a previously published protocol (Artus et al., 2010) (Fig. 1A). The genotype of individual XEN cell lines was confirmed by PCR after isolation and expansion, using primers specific for either *Nodal* or *LacZ*, which was knocked into the *Nodal* locus as part of the deletion strategy (Collignon et al., 1996) (Fig. 1B).

Wild type and $Nodal^{+/-}$ XEN cell lines were isolated at or above expected Mendelian ratios (12/48 (25%) and 32/48 (67%) respectively). By contrast, $Nodal^{-/-}$ XEN cell lines were isolated well below expected ratios ($n=4/48$; 8% as compared to 25% expected, $p=0.018$) (Fig. 1C). This suggests that *Nodal* expression in the embryo is required for optimal XEN cell derivation and/or maintenance.

Nodal mRNA levels were investigated in wild type and *Nodal* mutant XEN cell lines. Both wild type and $Nodal^{+/-}$ XEN cells expressed very low levels of *Nodal* when grown in the presence of LIF (Fig. 1D). However, this expression was rapidly lost after the removal of LIF from the medium (data not shown). In addition, since the mouse strain used for XEN cell isolation possessed a knock-in of the *LacZ* gene into the *Nodal* locus, XEN cell lines were stained for beta-galactosidase activity. The absence of beta-galactosidase activity corroborated the QRT-PCR data, demonstrating that *Nodal* is not expressed in these XEN cells (data not shown). These data are consistent with previous studies showing that wild type XEN cells do not express
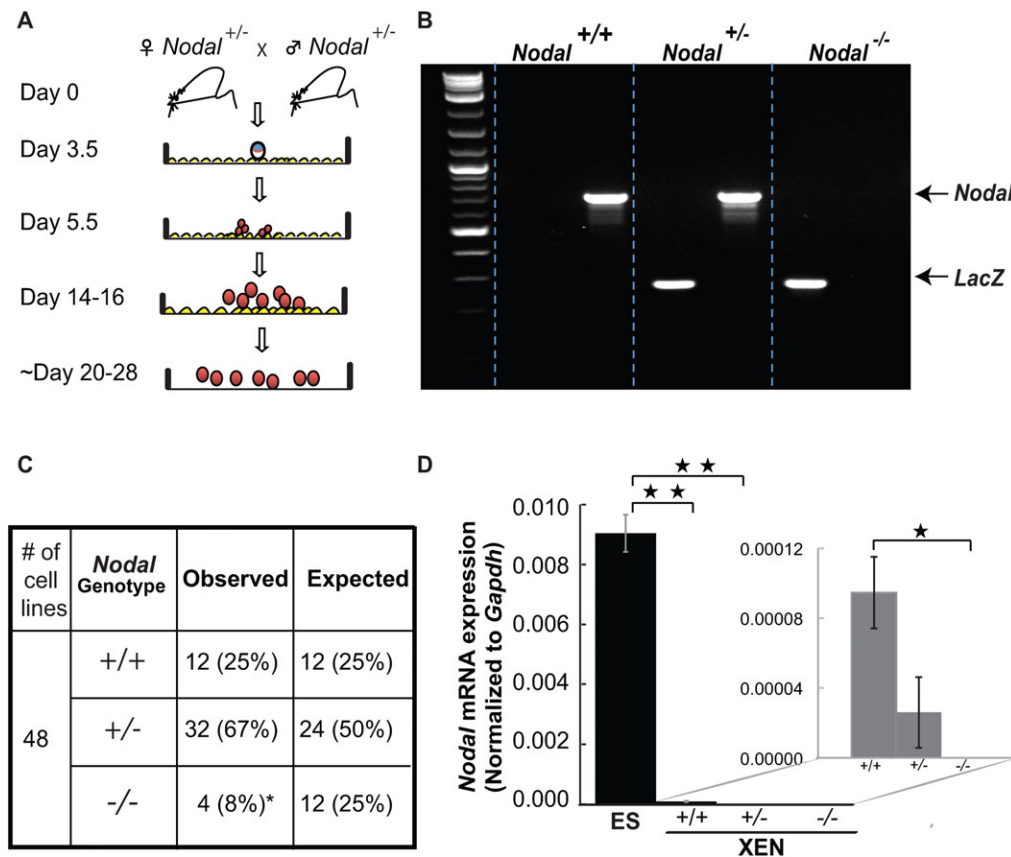
Fig. 1. **Derivation of murine blastocyst-derived eXtraembryonic ENdoderm (XEN) stem cells is impaired in the absence of *Nodal*.** (A) Schematic of the XEN cell derivation protocol. $Nodal^{+/-}$ mice were crossed on day 0. Blastocysts were collected on day 3.5 in M2 medium and cultured in 4-well gelatin-coated cell culture plates with mitotically inactivated MEFs. Outgrowths were disaggregated at 5.5 days into 2 to 3-cell clumps and replated. Colonies with characteristic XEN cell morphology appeared at day 20–28. (B) PCR genotyping of XEN cell lines. (C) $Nodal^{-/-}$ cell lines were not isolated at expected Mendelian ratios, only 4 of 48 cell lines (8%) were $Nodal^{-/-}$ in genotype as compared to 25% expected (p=0.018), while heterozygous and wild type XEN cell lines were isolated at or above expected Mendelian ratios. (D) QRT-PCR on cDNA synthesized from XEN cells. Relative *Nodal* expression was presented after normalization to *Gapdh*. Insert shows low levels of *Nodal* expression in $Nodal^{+/+}$ and $Nodal^{+/-}$ but not in $Nodal^{-/-}$ XEN cell lines. Error bars represent s.e.m. of three samples for each genotype (* indicates a p-value< 0.05, ** indicates a p-value< 0.006).

Nodal when expanded in the absence of LIF (Kunath et al., 2005; Brown et al., 2010b). Together, these findings also suggested that *Nodal* is not normally expressed in cultured XEN cells and is therefore not necessary for their survival, but is probably required for their derivation.

Nodal mutant XEN cells do not express pluripotency markers but do express markers for the primitive (PrE) and visceral endoderm (VE)

All of the cell lines that were identified, based on their morphology, as putative XEN cell lines, were confirmed as such by expression of the PrE/VE markers GATA4, GATA6, and SOX7. These markers were never detected in ES cells (Fig. 2A,B). Conversely, consistent with previous studies of wild type XEN cells (Kunath et al., 2005), *Nodal*$^{-/-}$ cell lines did not express the pluripotency marker OCT4, which was strongly expressed in ES cells. This was demonstrated by immunocytochemistry (Fig. 3A), Western blot (Fig. 3B), and QRT-PCR (Fig. 3C). Together, these data confirmed the identity of these cell lines as XEN cells and demonstrated that they were not contaminated with ES cells or any other pluripotent cell type that can be derived from mouse blastocysts.

Our previous studies demonstrated that XEN cells express markers for primitive, visceral and parietal endoderm. This study also described XEN cell morphology in some detail and noted that several distinct cellular morphologies were discernible in wild type XEN cells (Brown et al., 2010b). Interestingly, XEN cells isolated from *Nodal*$^{+/-}$ and *Nodal*$^{-/-}$ embryos were more

homogeneous in morphology than wild type XEN cells, and based on these morphological differences, cell lines of each of the three genotypes were readily distinguishable from the others (Fig. 3A and data not shown). Other studies have recently demonstrated that XEN cells become lineage restricted after the addition of specific growth factors (Artus et al., 2011; Julio et al., 2011), and one hallmark of this lineage restriction was a distinct change in the morphology of the XEN cells (Artus et al., 2011). To determine if the loss of *Nodal* during XEN cell isolation similarly impacted gene expression, the XEN cell lines were analyzed for quantitative changes in gene expression by QRT-PCR (Figs 2B, 4). *Gata4* and *Sox7* expression were highly sensitive to NODAL dosage since their expression was altered in both heterozygous and homozygous mutant cell lines. However, *Gata6* expression was only significantly increased in *Nodal*$^{-/-}$ cell lines. Based on our previous work, these data are consistent with an increase in VE fates within the *Nodal*$^{-/-}$ XEN cell lines (Brown et al., 2010b).

Nodal regulates anterior visceral endoderm (AVE) gene expression in XEN cells

Because previous studies had suggested a specific role for *Nodal* in regulating marker expression in the AVE (Brennan et al., 2001), we analyzed the AVE specific markers HEX, DKK1 and BMP2 (Madabhushi and Lacy, 2011), by immunocytochemistry, Western blot, and QRT-PCR. Both *Nodal*$^{-/-}$ and *Nodal*$^{+/-}$ XEN cells expressed higher levels of the AVE markers BMP2 and DKK1, while only *Nodal*$^{-/-}$ (but not *Nodal*$^{+/-}$) XEN cells
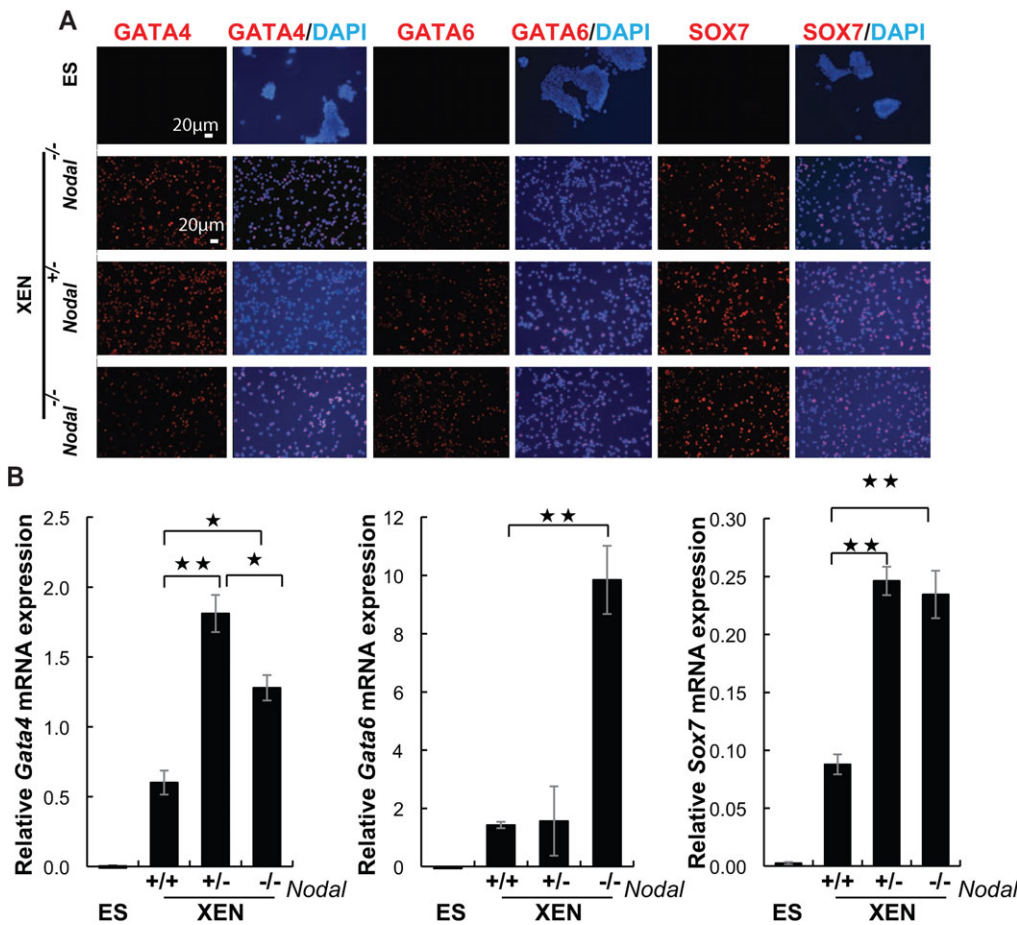
Fig. 2. **XEN cell lines derived from the *Nodal* mutant embryos express markers for the primitive and visceral endoderm.** Representative images of **(A)** immunocytochemistry for GATA4 (red), GATA6 (red) and SOX7 (red). Blue reveals DAPI staining of nuclei. Scale bar represents 20 μM. **(B)** QRT-PCR analysis for these same genes (* indicates a p-value< 0.05, ** indicates a p-value< 0.006).
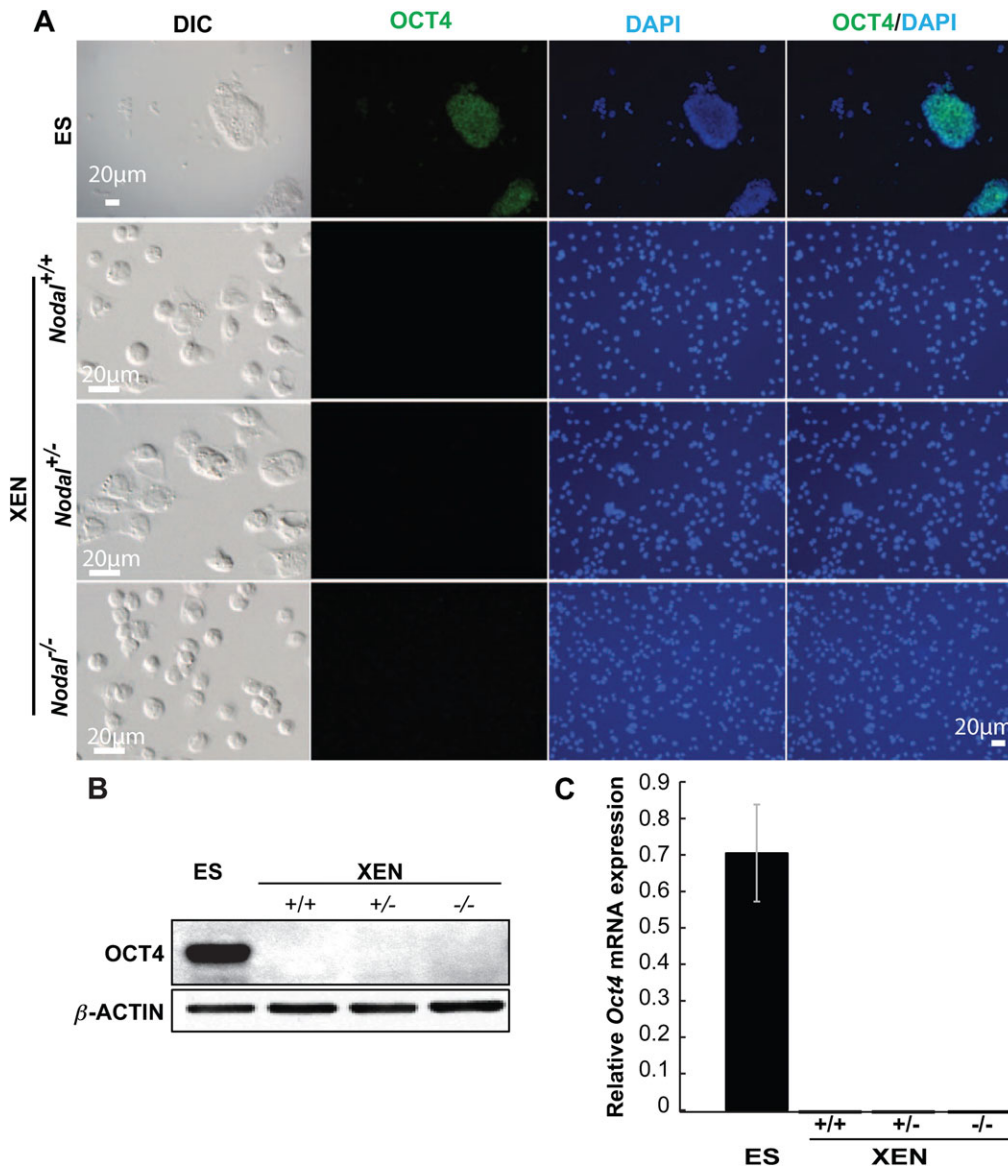
Fig. 3. XEN cell lines derived from the *Nodal* mutant embryos do not express the pluripotency marker OCT4. (A) Representative images of OCT4 (green) immunofluorescence in ES but not in XEN cells. Blue reveals DAPI staining of nuclei. Scale bars represents 20 µM. **(B)** Western blotting assay showing OCT4 detection in ES but not XEN cells. **(C)** QRT-PCR data showing *Oct4* mRNA expression in ES but not XEN cells.

expressed higher levels of the AVE marker HEX (Fig. 4). We also analyzed the expression of *Cerberus-like* and *Lefty1*; known targets of NODAL signaling in the AVE. Both markers were absent from XEN cells of all genotype (data not shown). These data demonstrated that *Nodal* negatively regulates the expression of a subset of AVE markers in XEN cells.

Medium conditioned by *Nodal* mutant XEN cells impacts the timing of cardiogenesis in EBs

AVE and AVE-like cell lines, including XEN cells, have been shown to increase cardiac differentiation from both nascent mesoderm and differentiating EBs (Arai et al., 1997; Mummery et al., 2003; Stary et al., 2005; Nijmeijer et al., 2009; Brown et al., 2010a). Since our data showed an upregulation of at least a subset of AVE markers in the $Nodal^{-/-}$ XEN cells, we hypothesized that these cells might possess enhanced cardiogenic potential as compared to wild type XEN cells. We previously showed that adding wild type XEN CM from days 4–6 of differentiation, increased cardiac formation within EBs (Brown et al., 2010a). Therefore, XEN CM collected from the

different genotypes ($Nodal^{+/+}$ XEN CM, $Nodal^{+/-}$ XEN CM or $Nodal^{-/-}$ XEN CM) was added to EB culture medium between days 4 and 6 of differentiation. The ES cells used in these studies possessed a *MHCα::*GFP reporter (Takahashi et al., 2003) that we previously validated as a faithful reporter for cardiomyocyte formation (Brown et al., 2010a). Cardiomyocyte differentiation was first evaluated by assessing the percentage of EBs that contained beating areas at each day of differentiation (Fig. 5A). EBs treated with $Nodal^{-/-}$ XEN CM or $Nodal^{+/-}$ XEN CM began beating on day 5 (with 18% and 2% beating, respectively). EBs treated with $Nodal^{+/+}$ XEN CM started beating on day 6. Finally EBs treated with control medium began beating on day 7. By day 14, there were no statistically significant differences among the four samples. Together these data suggest that the dosage of *Nodal* altered the characteristics XEN cells, which in turn, changed the way that XEN cells impacted the timing of cardiomyocyte differentiation.

By day14, EBs developed large areas of beating cardiomyocytes expressing GFP. Interestingly, the contracting loci that formed in response to $Nodal^{-/-}$ CM (Fig. 5B,
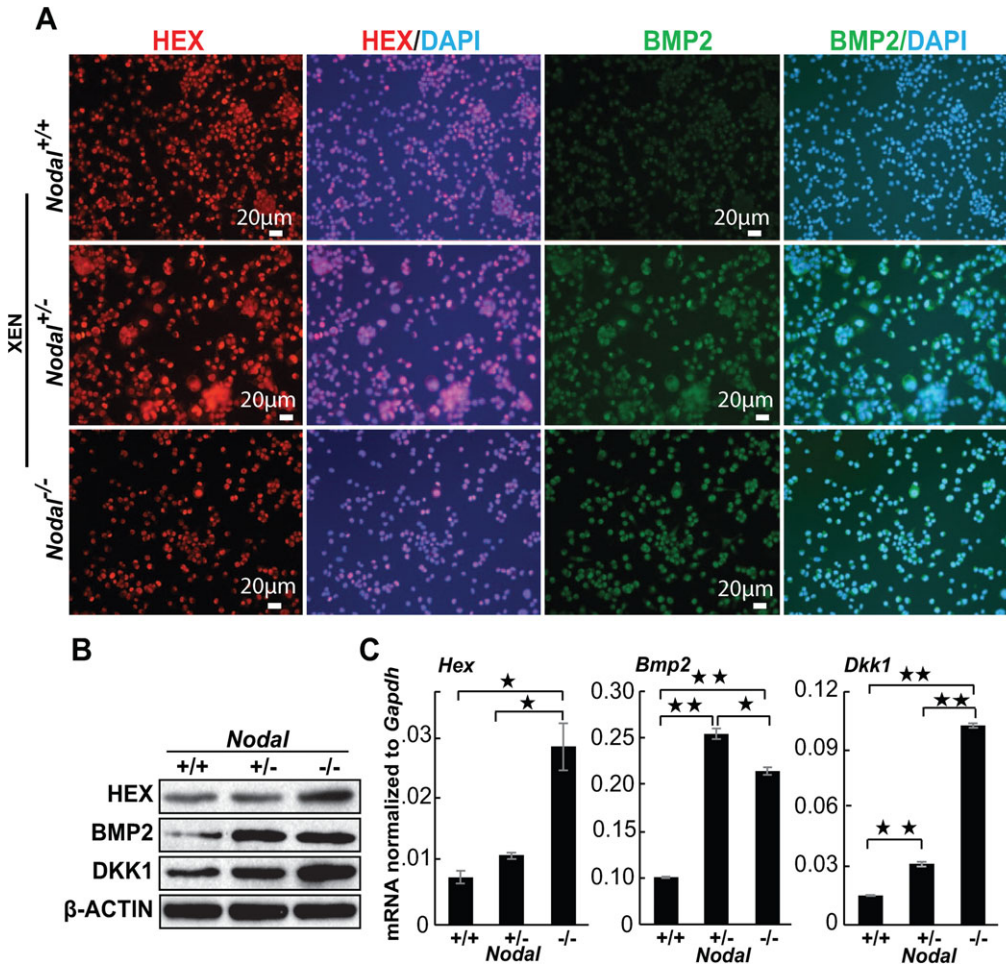
Fig. 4. Nodal regulates anterior visceral endoderm gene expression in XEN cells. (A) Representative images of immunocytochemistry analysis. HEX (red) and BMP2 (green) expression in XEN cells. Blue reveals DAPI staining of nuclei. XEN cells of all genotypes expressed HEX and BMP2. Scale bar represents 20 μM. **(B)** Western blot of HEX, BMP2, and DKK1 in XEN cells. **(C)** QRT-PCR analysis of *Hex*, *Bmp2*, and *Dkk1* mRNA expression in XEN cells. mRNA expression levels were presented after normalization to *Gapdh*. Error bars indicate s.e.m. (* indicates a p-value< 0.05, ** indicates a p-value< 0.006).

supplementary material Movie 1) appeared to be well organized as compared to untreated EBs (Fig. 5C, supplementary material Movie 2), with cardiomyocytes aligned in highly-organized, synchronously contracting sheets (supplementary material Movie 1). In contrast, contracting loci that formed in control EBs and those treated with wild type CM, appeared more disorganized with many areas within a single contractile region appearing to initiate contractions independently of one another (supplementary material Movie 2). These findings suggest that there is a higher degree of electrophysiological coupling in cardiomyocytes that develop from EBs treated with *Nodal* mutant CM and may suggest that these cells differentiate simultaneously. On the other hand, our data suggest that cardiomyocytes derived from either untreated EBs or EBs treated with wild type XEN CM may develop in several waves of differentiation.

To quantitatively compare overall cardiomyocyte differentiation between treated and untreated EBs, *MHCα* levels were investigated by QRT-PCR. *MHCα* expression peaked on day 7 in all samples, and mRNA levels were significantly increased in EBs treated with *Nodal*^{−/−} XEN CM. No change in *MHCα* expression was observed in response to *Nodal*^{+/+} XEN CM or *Nodal*^{+/−} XEN CM as compared to control EBs (Fig. 5D).

To quantify total myocardial differentiation after treatment with CM, EBs possessing the *MHCα*::GFP reporter (Takahashi et al., 2003) were treated as described above and analyzed by flow

cytometry on day 14 for overall cardiac formation. Unexpectedly, although EBs treated with *Nodal*^{−/−} XEN CM initiated cardiogenesis earlier and showed increased expression of *MHCα* on day 7 of differentiation, this treatment did not increase the total number of cardiomyocytes that formed as compared to controls. Instead, consistent with our previous findings (Brown et al., 2010a), EBs treated with wild type XEN CM showed an approximate 2-fold increase in overall cardiomyocyte differentiation (Fig. 5E).

Cardiac gene expression is delayed in EBs treated with *Nodal*^{+/+} XEN CM

Treatment of EBs with *Nodal*^{−/−} XEN CM caused earlier initiation of cardiogenesis, the formation of large, well-ordered beating areas and an increase in *MHCα* expression at day 7 of differentiation but with no subsequent increase in the total percentage of cardiomyocytes that formed. Based on these seemingly contradictory results, we hypothesized that *Nodal*^{−/−} XEN CM might cause a premature differentiation of cardiac progenitors with a subsequent depletion of the progenitor pool. The vertebrate heart develops from two sources of multipotent cardiac progenitors, the first heart field (FHF) and the second heart field (SHF) (Kelly et al., 2001; Cai et al., 2003; Meilhac et al., 2004; Zaffran et al., 2004; Waldo et al., 2005; Moretti et al., 2006; Abu-Issa and Kirby, 2007; Black, 2007; Qyang et al., 2007; Dyer and Kirby, 2009). FHF cells in the cardiac crescent express
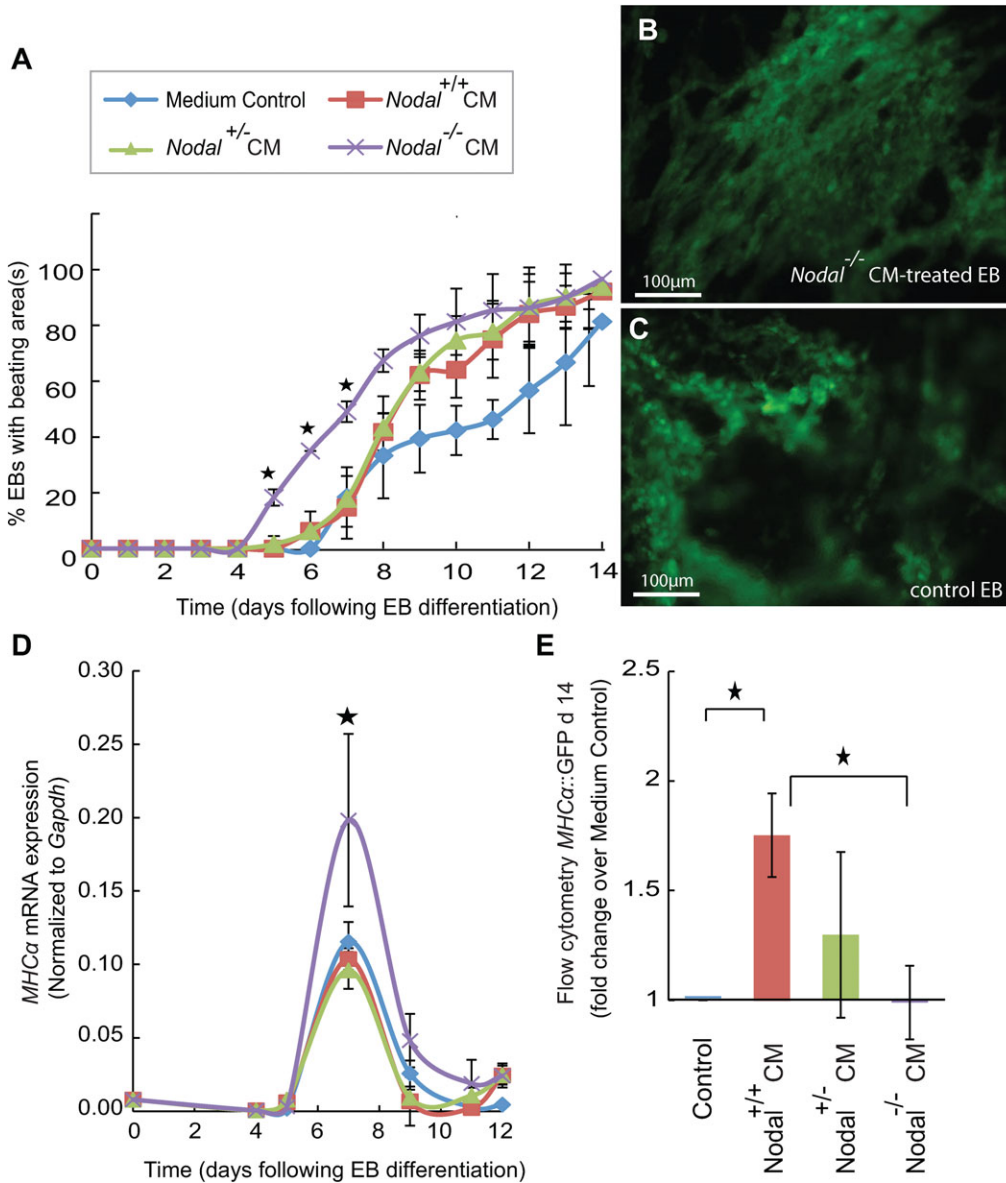
Fig. 5. Nodal impacts the initiation of cardiogenesis in embryoid bodies. Embryoid bodies (EBs) were treated between days 4 and 6 of differentiation with CM from XEN cells of all three genotypes (*Nodal*^{+/+} XEN CM, *Nodal*^{+/−} XEN CM, *Nodal*^{−/−} XEN CM), or medium control. **(A)** Beating EBs were counted and represented as a percentage of the total number of EBs counted. **(B,C)** Stills from supplementary material Movies 1 and 2, showing representative beating areas in EBs treated with *Nodal*^{+/−} XEN CM and control EBs, respectively. EBs express the *MHCα::*GFP reporter that indicates cardiomyocyte differentiation. Scale bar represent 100 μM. **(D)** *Myosin heavy chain alpha* (*MHCα*) mRNA expression (normalized to *Gapdh*) was examined in EBs by QRT-PCR. **(E)** Flow cytometry analysis on day 14 of cardiac differentiation comparing untreated EBs to those treated on days 4–6 with *Nodal* mutant XEN CM. EBs were made from CGR8 ES cells in which the *MHCα* promoter drives GFP protein expression upon cardiomyocyte formation. The percentage of MHCα expressing (GFP positive) cells were significantly increased in EBs treated with wild type XEN CM as compared to both controls and EBs treated with *Nodal*^{−/−} XEN CM. Error bars indicate s.e.m.(*indicates a p-value< 0.05).

Nkx2.5 and *Tbx5*, the latter of which is considered to be a more specific marker for the FHF, whereas *Nkx2.5* is expressed in both the FHF and SHF. At the cardiac crescent and linear heart tube stages, SHF cells, identified by the expression of *Islet-1* (Cai et al., 2003; Moretti et al., 2006; Qyang et al., 2007; Bu et al., 2009) and *Fgf10* (Kelly et al., 2001), reside adjacent to the FHF (Cai et al., 2003). Differentiation of SHF cells into myocardial cells is delayed for several days by a mechanism that is not well understood. The atria contain derivatives from both the FHF and the SHF. By comparison, the left ventricle develops primarily from the FHF and the right ventricle and outflow tract (OFT) primarily from SHF progenitors (Stennard et al., 2005; Vincent and Buckingham, 2010).

To assess whether endodermal signals impact one or both of these cardiac progenitor populations we assessed the expression of FHF and SHF markers by QRT-PCR over the course of EB differentiation with or without the addition of XEN CM. Untreated EBs typically showed two pulses of *Islet-1*

transcription over the first 12 days of EB differentiation (blue line, Fig. 6). By comparison, EBs treated with CM from wild type XEN cells had only a single, broader peak of *Islet-1* expression, the timing of which was delayed as compared to controls (red line, Fig. 6). Similarly, EBs treated with *Nodal*^{−/−} XEN CM also showed a single large peak of *Islet-1* expression, but in this case the peak was narrower and occurred earlier than the first peak in control EBs (purple line, Fig. 6). This finding suggested that CM from wild type XEN cells delayed the differentiation of *Islet-1* expressing cells, whereas CM from *Nodal*^{−/−} XEN cells caused *Islet-1* expressing cells to differentiate prematurely. Consistent with this, markers for differentiated cardiomyocytes including *Mlc2a, Hand1* and *Hand2* were all delayed in EBs treated with wild type CM (red lines, Fig. 6) but were initiated early in EBs treated with *Nodal*^{−/−} XEN CM (purple line, Fig. 6).

In contrast, *Tbx5* and *Nkx2.5* were also delayed in EBs treated with wild type XEN CM, but addition of *Nodal*^{−/−} XEN CM did
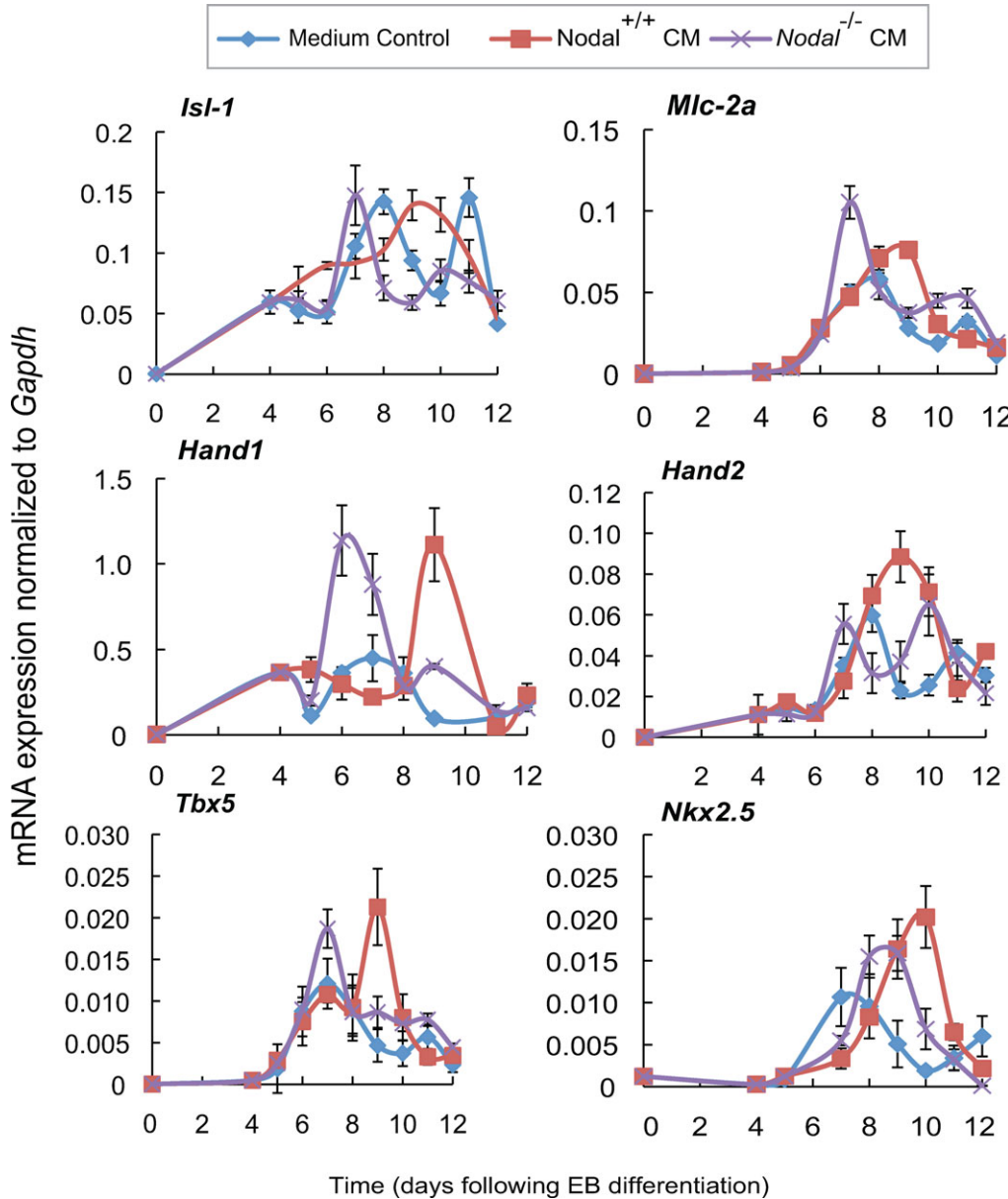
Fig. 6. Conditioned media from *Nodal* mutant XEN cells shifts the timing of cardiac gene expression in embryoid bodies (EBs). EBs were treated with *Nodal*^{+/+} XEN CM, *Nodal*^{−/−} XEN CM, or medium control from days 4 to 6 of differentiation. Cardiac genes were examined over the course of differentiation by QRT-PCR for expression of the cardiac progenitor marker, *Islet-1*, markers for differentiated cardiomyocytes, *Mlc2a*, *Hand1* and Hand2, and the early cardiac markers *Tbx5* and *Nkx2.5*. Relative mRNA expression was presented after normalization to *Gapdh*. Comparatively, EBs treated with *Nodal*^{+/+} XEN CM were shown to have a significant temporal shift in the onset of cardiac gene expression.

not cause premature activation of these markers. Rather, *Nodal*^{−/−} XEN CM had no effect on the timing of *Tbx5* and delayed the expression of *Nkx2.5* (purple line, Fig. 6). Therefore, the premature differentiation of cardiomyocytes observed in response to *Nodal*^{−/−} XEN CM is more likely to be due to a specific effect on *Islet-1* expressing cells rather than premature differentiation of cardiac progenitors in general. All of these markers were also assessed in EBs treated with *Nodal*^{+/−} XEN CM, but no differences were observed when compared to controls (Fig. 7). Together these findings suggest that a premature differentiation of *Islet-1* positive progenitors could account for the early differentiation of cardiomyocytes that we observed in EBs treated with *Nodal*^{−/−} XEN CM. Likewise, the increased number of cardiomyocytes observed when EBs were treated with wild type XEN CM could be accounted for by the delay discovered in the differentiation of cardiac progenitors. Furthermore, this delay may have allowed for increased proliferation of the progenitor pool.

In the embryo, the FHF contributes primarily to the left ventricle with a smaller contribution to the atria, whereas the SHF contributes to all lineages of the heart (but with a relatively small contribution to the left ventricle). If cardiac differentiation in EBs is equivalent to cardiac differentiation in the mouse embryo, we would expect that an early depletion of *Islet-1*expressing cells would lead to a general depletion of SHF derivatives and this should impact the ratio of atrial to ventricular cell types. Previous studies suggest that ES-derived cardiomyocytes begin to show electrophysiological maturation toward specific cardiac phenotypes 5–7 days after the onset of beating (Kolossov et al., 2005). To address whether premature differentiation of *Islet-1* progenitors might lead to a depletion of markers for the SHF and its derivatives, day 14 EBs (7+ days after the onset of beating) were analyzed for the expression of cardiac markers that become regionalized to specific chambers during development. To ensure that differences are due to changes in the regional expression of cardiac markers and not to
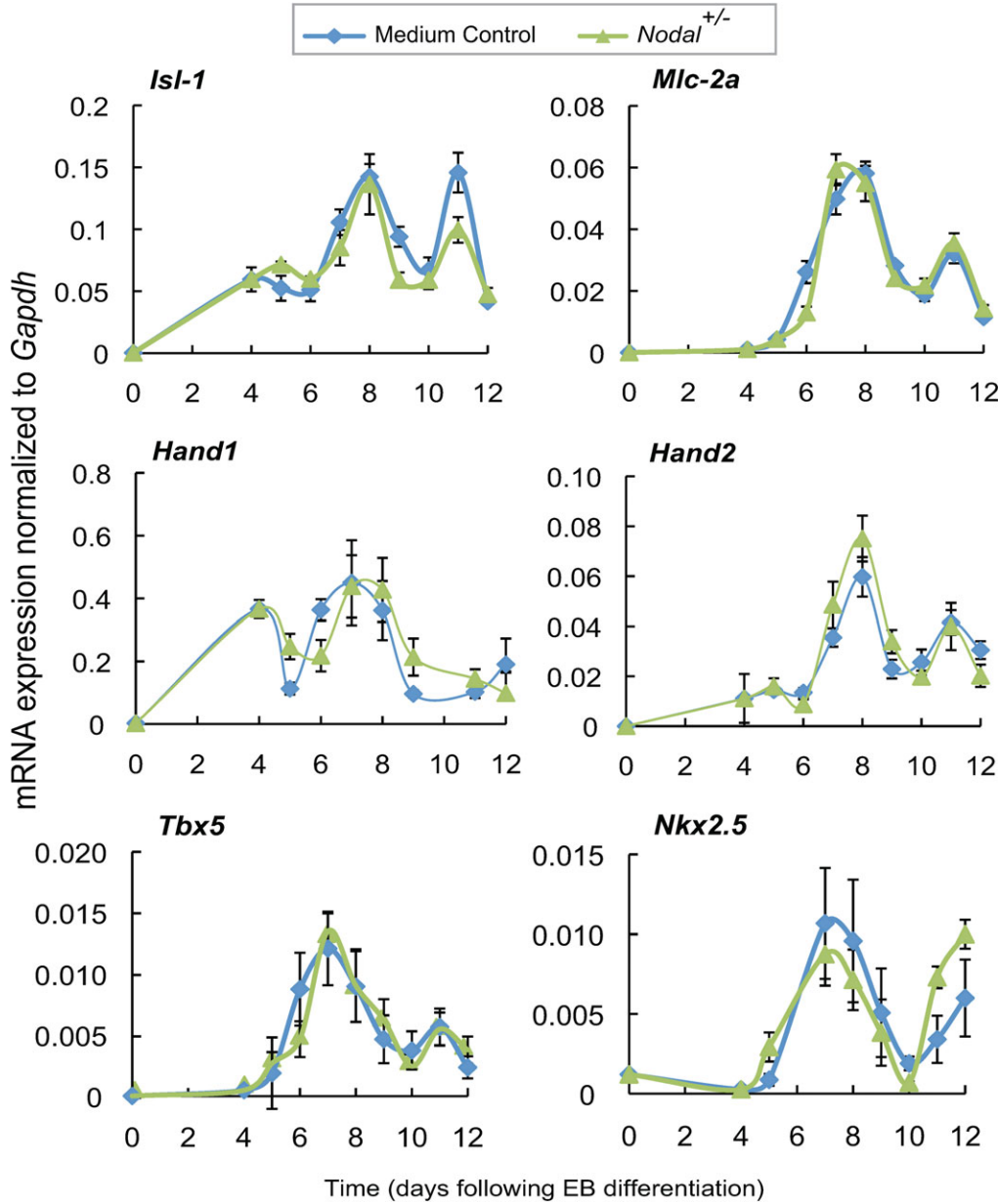
Fig. 7. Conditioned media from *Nodal*$^{+/-}$ XEN cells did not shift the timing of cardiac gene expression in EBs. EBs were treated with *Nodal*$^{+/-}$ XEN CM or medium control from days 4 to 6. Cardiac genes were examined over the course of differentiation by QRT-PCR for expression of the cardiac progenitor marker *Islet-1*, which marks the secondary heart field, the chamber specific markers *Mlc2a, Hand1* and *Hand2*, and the early cardiac markers *Tbx5* and *Nkx2.5*. Relative mRNA expression levels were presented after normalization to *Gapdh*. Comparatively, EBs treated with *Nodal*$^{+/-}$ XEN CM showed no significant changes in gene expression as compared to controls.

differences in overall cardiac induction, QRT-PCR data were normalized first to *Gapdh* and then to the general cardiac marker *Cardiac Troponin*. At day 14, *Mlc2a*, which becomes restricted to the atria, was expressed at significantly higher levels in untreated EBs and EBs treated with wild type CM as compared to those treated with *Nodal*$^{-/-}$ XEN CM. The average expression of *Anf* was also lower in EBs treated with *Nodal*$^{-/-}$ XEN CM. However, this marker was not informative because its expression was highly variable in untreated EBs. *Islet-1* and *Hand2,* which mark the SHF and SHF-derivatives respectively, were also significantly decreased in EBs treated with *Nodal*$^{-/-}$ XEN CM. There were no statistically significant differences in the expression of ventricular markers between EBs treated with wild type XEN CM and those treated with *Nodal* mutant XEN CM (Fig. 8). Taken together, these data are consistent with the idea that premature differentiation of cardiac progenitors leads to

a subsequent depletion of markers characteristic of the SHF and its derivatives.

Discussion

XEN cells allow for the molecular dissection of endodermal signals during heart induction

Signals from the AVE and its avian equivalent, the hypoblast, are required for the initial specification of cardiac cells in amniotes and mammals. In frogs, the DAE, that expresses the same markers as the AVE, is also required for early heart formation (Sater and Jacobson, 1989; Nascone and Mercola, 1995; Schneider and Mercola, 1999). In addition, signals from endodermal cell lines such as END2, PYS2 and XEN can mimic the effect of the AVE in vitro, enhancing cardiac differentiation from both ES cells and explants of undifferentiated mesoderm (Mummery et al., 2003; Stary et al.,
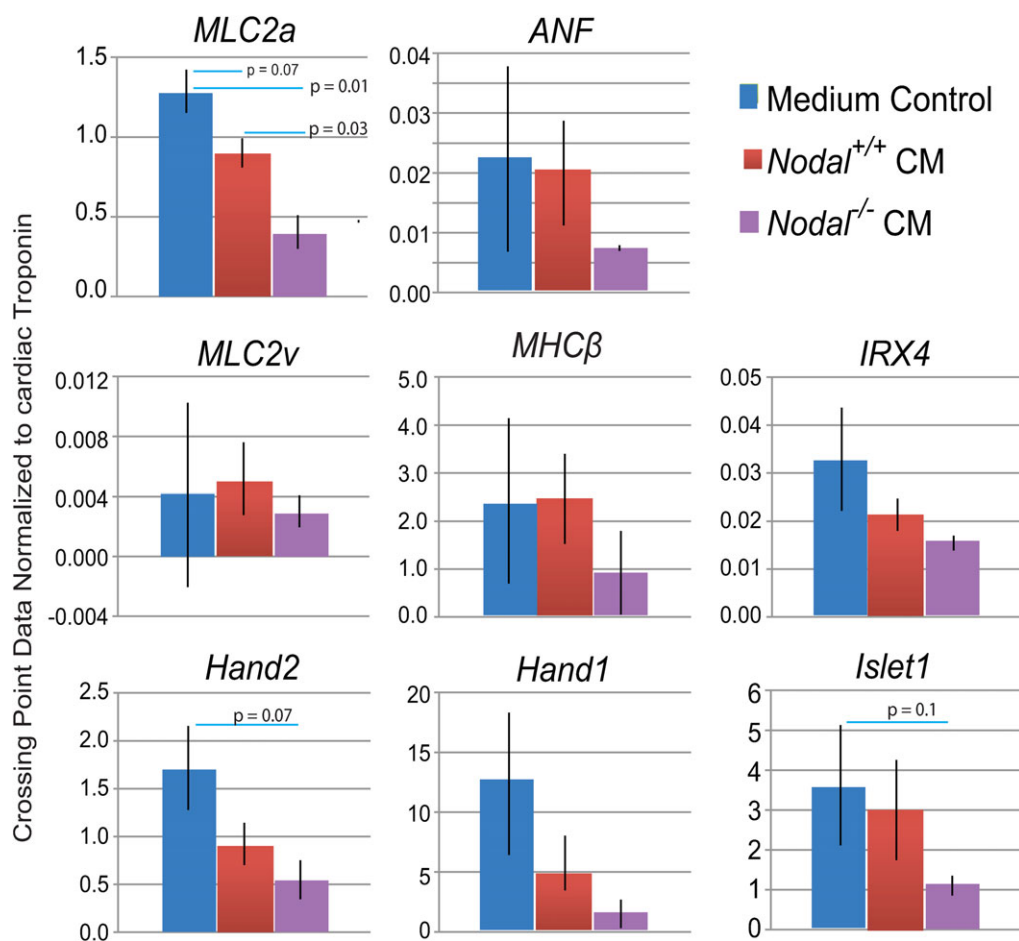
Fig. 8. Markers that become localized to specific cardiac chambers begin to be differentially expressed in day 14 EBs that were previously treated with *Nodal*$^{-/-}$ XEN CM. QRT-PCR data on day 14 of differentiation for markers that become regionalized to atrial or ventricular cardiomyocytes. Markers that become restricted to the ventricles (*Mlc2v*, *MHCβ*, *Irx4*) or which mark derivatives of the FHF in the embryo (*Hand1*) were not different between the two populations whereas those that become atrial-restricted (*Mlc2a*), mark the SHF (*Islet-1*) or mark derivatives of the SHF (*Hand2*) were expressed at lower levels in cells treated with *Nodal*$^{-/-}$ XEN CM. Error bars indicated s.e.m. Data considered significant had a p-value< 0.1.

2005; Nijmeijer et al., 2009; Brown et al., 2010a). Despite the importance of endodermal signals in myocardial differentiation, minimal progress has been made toward the identification of specific cardiogenic factors in the endoderm. In vivo, studies of endodermal signaling have been hampered by the small size and inaccessibility of gastrula stage mouse embryos. In vitro studies have also been slow because previous works have relied almost exclusively on embryonal carcinoma-derived cell lines that do not allow for the genetic ablation of candidate factors. Cell lines representing the primitive endoderm lineage (XEN cells) have recently been derived directly from blastocyst stage embryos (Kunath et al., 2005). Since XEN cells can be generated from both wild type and mutant strains, our recent finding that XEN CM promotes cardiogenesis (Brown et al., 2010a) suggests that they should provide a useful tool to study the role of endodermal signals in myocardial differentiation. To this end, we produced a *Nodal* mutant XEN cell line and assessed its ability to activate cardiogenesis as compared to wild type XEN cells.

Loss of *Nodal* results in the upregulation of a subset of AVE markers in XEN cells

A major finding of these studies is that loss of *Nodal* upregulated the expression of several AVE markers including HEX, DKK1 and BMP2 in XEN cells. This is surprising given that *Nodal* activates the expression of the AVE marker *Cerberus* in *Xenopus laevis* embryos (Foley et al., 2007) and is required for expression of the AVE marker *Lefty1* in mouse embryos (Brennan et al.,

2001). In addition, treatment of XEN cells with either recombinant NODAL or its co-factor CRIPTO resulted in an upregulation of *Cerberus-like* but not *Dkk1* or *Otx2* (Julio et al., 2011). These data suggest that redundant or parallel pathways pattern subsets of markers within the AVE such that NODAL regulates one set of markers (*i.e. Cerberus-like* and *Lefty*), while another set (*i.e. Bmp2*, *Hex*, *Otx2* and *Dkk1*) is repressed by NODAL and activated by a different pathway(s). Alternatively, recent studies suggest that cells expressing *Lefty* and *Cerberus-like* and those marked by *Hex*, may represent two distinct subgroups of cells within the AVE (Torres-Padilla et al., 2007; Takaoka et al., 2011).

While the mechanism for AVE marker upregulation in *Nodal*$^{-/-}$ XEN cells is still unclear, this finding suggested that they might possess superior cardiogenic potential as compared to wild type XEN cells. We had previously shown that conditioned medium from wild type XEN cells enhanced cardiac differentiation when it was added to growth medium from day 4 to 6 of EB differentiation (Brown et al., 2010a). By comparison to both control EBs and those treated with wild type XEN CM, *Nodal*$^{-/-}$ XEN CM did not enhance overall cardiac differentiation but did result in both earlier beating and increased expression of *MHCα* mRNA on day 7 of differentiation. To clarify these conflicting findings, we investigated the effect of CM on the expression of cardiac progenitor markers. In EBs treated with wild type XEN CM, *Islet-1* expression was delayed as compared to controls, whereas

EBs treated with *Nodal*$^{-/-}$ XEN CM showed a premature increase in the expression of *Islet-1* as compared to controls. Two other cardiac progenitor markers, *Nkx2.5* and *Tbx5,* were either unaffected or slightly delayed in response to *Nodal*$^{-/-}$ XEN CM. While there is no clear definition of FHF and SHF within EBs, our observation demonstrate that markers associated with the FHF (*Nkx2.5* and *Tbx5*) and SHF (*Islet-1*) respond differently to endodermal signals. Prall and colleagues proposed a model to explain how the embryo regulates the switch from FHF and SHF differentiation involving a negative feed back loop comprised of *Nkx2.5*, *Bmp2* and SMAD-1. In the absence of *Nkx2.5*, they saw an upregulation of *Bmp2* and SMAD phosphorylation, and this resulted in a premature differentiation of *Islet-1* positive cells, with a subsequent failure of SHF derivatives to proliferate. Similarly, in these studies we saw an upregulation of BMP2, premature expression of *Islet-1* and a failure of the cardiac pool to expand. By day 14, we also observed a significant decrease in markers for the SHF and its derivatives within EBs.

Notably, Prall and colleagues observed that the failure of SHF progenitors to proliferate in *Nkx2.5* null embryos led to the formation of a malformed heart containing a single ventricle and a severely truncated OFT (Prall et al., 2007). Consistent with this, mice in which an enhancer of early *Nodal* expression is knocked out, had normal cardiac specification but subsequent heart defects including ventricular septal defects and misplacement of the outflow tract (Norris et al., 2002). In addition, many human congenital heart defects including Tetralogy of Fallot, that are thought to be related to defects in SHF development, have been linked to specific mutations at the *Nodal* locus (Roessler et al., 2009). Our data suggests that endodermal signals that are regulated by *Nodal* may mediate the time of the embryos switch from FHF to SHF development.

Nodal is not the direct cardiogenic signal

Both wild type and *Nodal* heterozygous mutant XEN cells expressed very low levels of *Nodal* mRNA when grown in the presence of LIF. However, this expression was rapidly lost after the removal of LIF from the media. In addition, we previously showed that wild type XEN cells, grown in the absence of LIF possessed cardiogenic potential despite the fact that they expressed no Nodal (Brown et al., 2010b). These findings suggest that the cardiogenic potential of XEN cells is not due to

Nodal signaling from the XEN cells themselves, but is an indirect consequence of *Nodal*'s ability to pattern XEN cells. These XEN cells are most likely patterned during the initial phases of isolation when the primitive endoderm and epiblast cells remain in culture. More specifically, these data suggest that genes regulated by *Nodal* in the endoderm may be required to maintain SHF progenitors in pre-cardiac state.

Materials and Methods

Derivation and culture of *Nodal* mutant XEN cell lines

Mice carrying a *Nodal*^{LacZ} allele (Collignon et al., 1996) were maintained on an ICR genetic background. *Nodal*$^{LacZ/+}$ mice were crossed to obtain *Nodal*$^{LacZ/LacZ}$ embryos (referred to in the text as *Nodal*$^{-/-}$). XEN cell lines were derived from these embryos according to a previously described method (Kunath et al., 2005; Artus et al., 2010) (Fig. 1A). After 2–3 weeks, colonies with XEN cell morphology were observed in over half the cultures. The colonies were expanded onto gelatinized 10 cm plates with mouse embryonic fibroblasts (MEFs). After passaging off MEFs, genomic DNA was purified from cell pellets using DNeasy Blood & Tissue Kit (QIAGEN) and putative XEN cells lines were genotyped using previously described primer sequences (Collignon et al., 1996) (Table 1).

XEN cells were maintained on MEFs in DMEM supplemented with 20% fetal bovine serum (FBS; GIBCO), 1 mM sodium pyruvate (Mediatech), 2 mM L-glutamine (Mediatech), 50 mg/ml penicillin/streptomycin (Cellgro), 55 mM β-mercaptoethanol (Sigma), 100 mM non-essential amino acids (Mediatech), and 1000 units/ml of ESGRO (LIF) (Millipore).

To collect CM, XEN cells (no MEFs), were cultured in media without LIF. Media were conditioned with *Nodal*$^{+/+}$ XEN cells (*Nodal*$^{+/+}$ XEN CM), *Nodal*$^{+/-}$ XEN cells (*Nodal*$^{+/-}$ XEN CM), or *Nodal*$^{-/-}$ XEN cells (*Nodal*$^{-/-}$ XEN CM) and incubated at 37℃, 5% CO_2. Medium control consisted of medium that was not conditioned by XEN cells. After 24-hour incubation, media were sterile filtered and stored at −20℃ for later use.

Culture and differentiation of ES cells

Mouse R1 or CGR8 embryonic stem (ES) cells were cultured and differentiated as previously described (Brown et al., 2010a). For in vitro differentiation, ES cells were passaged off MEFs then plated as hanging drops at a concentration of 15,000 cells/mL (300 cells per hanging drop) in Iscove's Modified Dulbecco Medium (IMDM; Gibco), supplemented with 20% serum (Gibco), 50 mg/mL each of penicillin/streptomycin (100 units/mL and 100 μg/mL, respectively) (Cellgro), 200 mg/mL apo-transferrin (Sigma), 5% protein-free hybridoma medium (PFHMII; Gibco), 0.5 mM 1-thioglycerol (Sigma), and 0.5 mM ascorbic acid (Sigma).

Immunocytochemistry

Cells were plated onto gelatinized chamber slides. Immunocytochemistry was performed at various degrees of confluence to ensure that there were no changes in gene expression resulting from cell density (data not shown). The cells were fixed in 4% paraformaldehyde at room temperature then permeabilized with 0.25% Triton X-100-PBS at room temperature. Blocking was carried out with 10% heat-inactivated FBS-0.25% Triton X-100 in PBS at room temperature then incubated with primary antibody overnight at 4℃. After this, cells were incubated with

Table 1. QRT-PCR primers used in this study. Primers were designed for detecting murine gene expression.

Gene name	Forward primer	Reverse primer
LacZ	5′-GTC GTT TTA CAA CGT CGT GAC T-3′	5′-GAT GGG CGC ATC GTA ACC GTG C-3′
Nodal	5′-ATG TGG ACG TGA CCG GAC AGA ACT-3′	5′-CTG GAT GTA GGC ATG GTT GGT AGG AT-3′
Oct4	5′-TCA GCT TGG GCT AGA GAA GG-3′	5′-TGA CGG GAA CAG AGG GAA AG-3′
Gata4	5′-CAT CAA ATC GCA GCC T-3′	5′-AAG CAA GCT AGA GTC CT-3′
Gata6	5′-ACC ATC ACC CGA CCT ACT CG-3′	5′-CGA CAG GTC CTC CAA CAG GT-3′
Sox7	5′-CAA GGA TGA GAG GAA ACG TCT G-3′	5′-TCA TCC ACA TAG GGT CTC TTC TG-3′
Hex	5′-GGA GGC TGA TCT TGA CT-3′	5′-GTA GGG ACT GCG TCA T-3′
Bmp2	5′-GAG AAC ACC CGG AGA AGG AG-3′	5′-TGG GGA AGC AGC AAC ACT A-3′
Dkk1	5′-TAC AAT GAT GGC TCT CTG CAG CCT-3′	5′-TGG TCA GAG GGC ATG CAT ATT CCA-3′
MHCα	5′-CAT GCC AAT GAC GAC CT-3′	5′-CCT ACA CTC CTG TAC TGC C-3′
Tbx5	5′-CCA GCT CGG CGA AGG GAT GTT T-3′	5′-CCG ACG CCG TGT ACC GAG TGA T-3′
Isl-1	5′-GAG TCA TCC GAG TGT GGT TTC-3′	5′-ACC ATG GGA GTT CCT GTC ATC-3′
Nkx2.5	5′-TTA CC GGG AGC CTA CGG TG-3′	5′-GCT TTC CGT CGC CGC CGT GCG CGT G-3′
Hand1	5′-CCG CCT GCC CAA ACG AAA AG-3′	5′-CCG AGG CAG GAG GGA AGC-3′
Hand2	5′-CCA GAT ACA TCG CCT ACC TC-3′	5′-TTC TTG TCG TTG CTG CTC AC-3′
Mlc-2a	5′-CAG ACC TGA AGG AGA CCT ATT CC-3′	5′-CTA CCT CAG CAG GAG AGA ACT TG-3′
Gapdh	5′-AAT GGA TAC GGC TAC AGC-3′	5′- GTG CAG CGA ACT TTA TTG-3′

Biology Open

secondary antibody and counterstained with DAPI. Primary antibodies used were: OCT4 (1:250; Cell Signaling), GATA4 (1:1000; Santa Cruz), GATA6 (1:500; R&D systems), SOX7 (1:500; R&D systems), BMP2 (1:250; Abcam), and HEX (1:500; Abcam). Staining was detected by Alexa Fluor 555-conjugated anti-goat antibody (1:1000; Invitrogen), Alexa Fluor 555-conjugated anti-rabbit antibody (1:1000; Invitrogen), Alexa Fluor 555-conjugated anti-mouse antibody (1:1000; Invitrogen), or Alexa Fluor 488-conjugated anti-mouse antibody (1:1000; Invitrogen).

Western blot

Whole cell extracts (20 mg) were prepared using RIPA lysis buffer, electrophoresed through 4–20% NuPAGE Bis-Tris gel (Invitrogen), transferred to a PVDF membrane (Pall Life Sciences) and blotted by standard techniques. Primary antibodies used were: OCT4 (1:1000; Cell Signaling), GATA4 (1:1000; Santa Cruz), GATA6 (1:1000; R&D systems), SOX7 (1:1000; R&D systems), BMP2 (1:200; Abcam), DKK1 (1:200; Santa Cruz), and HEX (1:200; Abcam). Secondary antibodies were anti-mouse HRP (1:3000; Cell Signaling), anti-rabbit HRP (1:3000; GE Healthcare). As a loading control, membranes were stripped and probed with anti-ACTIN (1:2000; Santa Cruz) and labeled with anti-goat HRP (1:10,000; Santa Cruz). Chemoluminescent detection (Thermo Scientific) was performed according to the manufacturer's instructions.

RNA isolation, reverse transcription, and QRT-PCR analysis

Total RNA from cells was isolated with Tri-Reagent (Sigma). First strand cDNA synthesis was performed with 1 µg of total RNA using QuantiTect Reverse Transcription kit (QIAGEN). cDNAs were analyzed by QRT-PCR for the expression of *Nodal, Oct4, Gata4, Gata6, Sox7, Hex, Dkk1, Bmp2, Tbx5, Islet-1, Nkx2.5, Mlc2a, Hand1,* and *Hand2* (Table 1). QRT-PCR was performed on a Roche Lightcycler 480, and analysis was done with the Roche Lightcycler 480 software package. Crossing point data was corrected for primer efficiency (as determined by analysis of a standard dilution curve for a positive control) then normalized to expression of *Gapdh*.

Flow cytometry

CGR8 ES cells expressing the Green Fluorescent Protein (GFP) reporter under the *Myosin Heavy Chain-alpha* (*MHCα*) promoter (*MHCα::*GFP) (Takahashi et al., 2003) were used to form EBs. EBs were dissociated with trypsin. Acquisition and analysis for amount of GFP positive cells was performed on a BD FACSCalibur cytometer (BD Biosciences) with the aid of the BD Cell Quest software.

Statistical Analysis

The statistical significance of differences among treatment groups was assessed with Scheffe multiple-comparison test. Error bars indicate standard error. (s.e.m.). Differences were considered significant at p-value< 0.05 (a p-value< 0.05 is indicated by one star, p-value< 0.006 is indicated by two stars in figures). Significance of regional cardiac markers was determined by unpaired two-tailed *t*-test. Differences were considered significant at a p-value< 0.1.

Competing Interests

There is no potential competing conflict of interests in connection with this manuscript. All sources of financial support for this study have been disclosed and are indicated in the acknowledgements.

Acknowledgements

References

Abu-Issa, R. and Kirby, M. L. (2007). Heart field: from mesoderm to heart tube. *Annu. Rev. Cell Dev. Biol.* 23, 45-68.

Arai, A., Yamamoto, K. and Toyama, J. (1997). Murine cardiac progenitor cells require visceral embryonic endoderm and primitive streak for terminal differentiation. *Dev. Dyn.* 210, 344-353.

Artus, J., Panthier, J. J. and Hadjantonakis, A. K. (2010). A role for PDGF signaling in expansion of the extra-embryonic endoderm lineage of the mouse blastocyst. *Development* 137, 3361-3372.

Artus, J., Douvaras, P., Piliszek, A., Isern, J., Baron, M. H. and Hadjantonakis, A. K. (2012). BMP4 signaling directs primitive endoderm-derived XEN cells to an extraembryonic visceral endoderm identity. *Dev. Biol.* 361, 245-262.

Black, B. L. (2007). Transcriptional pathways in second heart field development. *Semin. Cell Dev. Biol.* 18, 67-76.

Brennan, J., Lu, C. C., Norris, D. P., Rodriguez, T. A., Beddington, R. S. and Robertson, E. J. (2001). Nodal signalling in the epiblast patterns the early mouse embryo. *Nature* 411, 965-969.

Brown, K., Doss, M. X., Legros, S., Artus, J., Hadjantonakis, A. K. and Foley, A. (2010a). eXtraembryonic ENdoderm (XEN) Cells Produce Factors that Activate Heart Formation. *PLoS ONE* 5, e13446.

Brown, K., Legros, S., Artus, J., Doss, M. X., Khanin, R., Hadjantonakis, A. K. and Foley, A. (2010b). A comparative analysis of extra-embryonic endoderm cell lines. *PLoS ONE* 5, e12016.

Bu, L., Jiang, X., Martin-Puig, S., Caron, L., Zhu, S., Shao, Y., Roberts, D. J., Huang, P. L., Domian, I. J. and Chien, K. R. (2009). Human ISL1 heart progenitors generate diverse multipotent cardiovascular cell lineages. *Nature* 460, 113-117.

Cai, C. L., Liang, X., Shi, Y., Chu, P. H., Pfaff, S. L., Chen, J. and Evans, S. (2003). Isl1 identifies a cardiac progenitor population that proliferates prior to differentiation and contributes a majority of cells to the heart. *Dev. Cell* 5, 877-889.

Camus, A., Perea-Gomez, A., Moreau, A. and Collignon, J. (2006). Absence of Nodal signaling promotes precocious neural differentiation in the mouse embryo. *Dev. Biol.* 295, 743-755.

Collignon, J., Varlet, I. and Robertson, E. J. (1996). Relationship between asymmetric *nodal* expression and the direction of embryonic turning. *Nature* 381, 155-158.

David, N. B. and Rosa, F. M. (2001). Cell autonomous commitment to an endodermal fate and behaviour by activation of Nodal signalling. *Development* 128, 3937-3947.

Dyer, L. A. and Kirby, M. L. (2009). The role of secondary heart field in cardiac development. *Dev. Biol.* 336, 137-144.

Foley, A. C., Korol, O., Timmer, A. M. and Mercola, M. (2007). Multiple functions of Cerberus cooperate to induce heart downstream of Nodal. *Dev. Biol.* 303, 57-65.

Fullilove, S. L. (1970). Heart induction: distribution of active factors in newt endoderm. *J. Exp. Zool.* 175, 323-326.

Granier, C., Gurchenkov, V., Perea-Gomez, A., Camus, A., Ott, S., Papanayotou, C., Iranzo, J., Moreau, A., Reid, J., Koentges, G. et al. (2011). Nodal cis-regulatory elements reveal epiblast and primitive endoderm heterogeneity in the peri-implantation mouse embryo. *Dev. Biol.* 349, 350-362.

Holtzinger, A., Rosenfeld, G. E. and Evans, T. (2010). Gata4 directs development of cardiac-inducing endoderm from ES cells. *Dev. Biol.* 337, 63-73.

Jacobson, A. G. (1960). Influences of ectoderm and endoderm on heart differentiation in the newt. *Dev. Biol.* 2, 138-154.

Julio, M. K., Alvarez, M. J., Galli, A., Chu, J., Price, S. M., Califano, A. and Shen, M. M. (2011). Regulation of extra-embryonic endoderm stem cell differentiation by Nodal and Cripto signaling. *Development* 138, 3885-3895.

Kelly, R. G., Brown, N. A. and Buckingham, M. E. (2001). The arterial pole of the mouse heart forms from Fgf10-expressing cells in pharyngeal mesoderm. *Dev. Cell* 1, 435-440.

Kolossov, E., Lu, Z., Drobinskaya, I., Gassanov, N., Duan, Y., Sauer, H., Manzke, O., Bloch, W., Bohlen, H., Hescheler, J. et al. (2005). Identification and characterization of embryonic stem cell-derived pacemaker and atrial cardiomyocytes. *FASEB J.* 19, 577-579.

Kunath, T., Arnaud, D., Uy, G. D., Okamoto, I., Chureau, C., Yamanaka, Y., Heard, E., Gardner, R. L., Avner, P. and Rossant, J. (2005). Imprinted X-inactivation in extra-embryonic endoderm cell lines from mouse blastocysts. *Development* 132, 1649-1661.

Lough, J. and Sugi, Y. (2000). Endoderm and heart development. *Dev. Dyn.* 217, 327-342.

Madabhushi, M. and Lacy, E. (2011). Anterior Visceral Endoderm Directs Ventral Morphogenesis and Placement of Head and Heart via BMP2 Expression. *Dev. Cell* 21, 907-919.

Marvin, M. J., Di Rocco, G., Gardiner, A., Bush, S. M. and Lassar, A. B. (2001). Inhibition of Wnt activity induces heart formation from posterior mesoderm. *Genes Dev.* 15, 316-327.

Meilhac, S. M., Esner, M., Kelly, R. G., Nicolas, J. F. and Buckingham, M. E. (2004). The clonal origin of myocardial cells in different regions of the embryonic mouse heart. *Dev. Cell* 6, 685-698.

Mesnard, D., Guzman-Ayala, M. and Constam, D. B. (2006). Nodal specifies embryonic visceral endoderm and sustains pluripotent cells in the epiblast before overt axial patterning. *Development* 133, 2497-2505.

Moretti, A., Caron, L., Nakano, A., Lam, J. T., Bernshausen, A., Chen, Y., Qyang, Y., Bu, L., Sasaki, M., Martin-Puig, S. et al. (2006). Multipotent embryonic isl1+ progenitor cells lead to cardiac, smooth muscle, and endothelial cell diversification. *Cell* 127, 1151-1165.

Mummery, C., Ward-van Oostwaard, D., Doevendans, P., Spijker, R., van den Brink, S., Hassink, R., van der Heyden, M., Opthof, T., Pera, M., de la Riviere, A. B. et al. (2003). Differentiation of human embryonic stem cells to cardiomyocytes: role of coculture with visceral endoderm-like cells. *Circulation* 107, 2733-2740.

Nascone, N. and Mercola, M. (1995). An inductive role for the endoderm in *Xenopus* cardiogenesis. *Development* 121, 515-523.

Nijmeijer, R. M., Leeuwis, J. W., DeLisio, A., Mummery, C. L. and Chuva de Sousa Lopes, S. M. (2009). Visceral endoderm induces specification of cardiomyocytes in mice. *Stem Cell Res.* 3, 170-178.

Norris, D. P., Brennan, J., Bikoff, E. K. and Robertson, E. J. (2002). The Foxh1-dependent autoregulatory enhancer controls the level of Nodal signals in the mouse embryo. *Development* **129**, 3455-3468.

Orts-Llorca, F. and Gil, D. R. (1965). Influence of the endoderm on heart differentiation. *Roux's Arch. EntwMech. Org.* **156**, 368-370.

Prall, O. W., Menon, M. K., Solloway, M. J., Watanabe, Y., Zaffran, S., Bajolle, F., Biben, C., McBride, J. J., Robertson, B. R., Chaulet, H. et al. (2007). An Nkx2-5/Bmp2/Smad1 negative feedback loop controls heart progenitor specification and proliferation. *Cell* **128**, 947-959.

Qyang, Y., Martin-Puig, S., Chiravuri, M., Chen, S., Xu, H., Bu, L., Jiang, X., Lin, L., Granger, A., Moretti, A. et al. (2007). The renewal and differentiation of Isl1+ cardiovascular progenitors are controlled by a Wnt/beta-catenin pathway. *Cell Stem Cell* **1**, 165-179.

Roessler, E., Pei, W., Ouspenskaia, M. V., Karkera, J. D., Velez, J. I., Banerjee-Basu, S., Gibney, G., Lupo, P. J., Mitchell, L. E., Towbin, J. A. et al. (2009). Cumulative ligand activity of NODAL mutations and modifiers are linked to human heart defects and holoprosencephaly. *Mol. Genet. Metab.* **98**, 225-234.

Sater, A. K. and Jacobson, A. G. (1989). The specification of heart mesoderm occurs during gastrulation in *Xenopus laevis*. *Development* **105**, 821-830.

Schneider, V. A. and Mercola, M. (1999). Spatially distinct head and heart inducers within the *Xenopus* organizer region. *Curr. Biol.* **9**, 800-809.

Stary, M., Pasteiner, W., Summer, A., Hrdina, A., Eger, A. and Weitzer, G. (2005). Parietal endoderm secreted SPARC promotes early cardiomyogenesis in vitro. *Exp. Cell Res.* **310**, 331-343.

Stennard, F. A., Costa, M. W., Lai, D., Biben, C., Furtado, M. B., Solloway, M. J., McCulley, D. J., Leimena, C., Preis, J. I., Dunwoodie, S. L. et al. (2005). Murine T-box transcription factor Tbx20 acts as a repressor during heart development, and is essential for adult heart integrity, function and adaptation. *Development* **132**, 2451-2462.

Sugi, Y. and Lough, J. (1994). Anterior endoderm is a specific effector of terminal cardiac myocyte differentiation of cells from the embryonic heart forming region. *Dev. Dyn.* **200**, 155-162.

Takahashi, T., Lord, B., Schulze, P. C., Fryer, R. M., Sarang, S. S., Gullans, S. R. and Lee, R. T. (2003). Ascorbic acid enhances differentiation of embryonic stem cells into cardiac myocytes. *Circulation* **107**, 1912-1916.

Takaoka, K., Yamamoto, M. and Hamada, H. (2011). Origin and role of distal visceral endoderm, a group of cells that determines anterior-posterior polarity of the mouse embryo. *Nat. Cell Biol.* **13**, 743-752.

Tonegawa, A., Moriya, M., Tada, M., Nishimatsu, S., Katagiri, C. and Ueno, N. (1996). Heart formative factor(s) is localized in the anterior endoderm of early *Xenopus* neurula. *Roux's Arch. Dev. Biol.* **205**, 282-289.

Torres-Padilla, M. E., Richardson, L., Kolasinska, P., Meilhac, S. M., Luetke-Eversloh, M. V. and Zernicka-Goetz, M. (2007). The anterior visceral endoderm of the mouse embryo is established from both preimplantation precursor cells and by de novo gene expression after implantation. *Dev. Biol.* **309**, 97-112.

Varlet, I., Collignon, J. and Robertson, E. J. (1997). nodal expression in the primitive endoderm is required for specification of the anterior axis during mouse gastrulation. *Development* **124**, 1033-1044.

Vincent, S. D. and Buckingham, M. E. (2010). How to make a heart: the origin and regulation of cardiac progenitor cells. *Curr. Top. Dev. Biol.* **90**, 1-41.

Waldo, K. L., Hutson, M. R., Ward, C. C., Zdanowicz, M., Stadt, H. A., Kumiski, D., Abu-Issa, R. and Kirby, M. L. (2005). Secondary heart field contributes myocardium and smooth muscle to the arterial pole of the developing heart. *Dev. Biol.* **281**, 78-90.

Yamamoto, M., Saijoh, Y., Perea-Gomez, A., Shawlot, W., Behringer, R. R., Ang, S. L., Hamada, H. and Meno, C. (2004). Nodal antagonists regulate formation of the anteroposterior axis of the mouse embryo. *Nature* **428**, 387-392.

Yuasa, S., Itabashi, Y., Koshimizu, U., Tanaka, T., Sugimura, K., Kinoshita, M., Hattori, F., Fukami, S., Shimazaki, T., Ogawa, S. et al. (2005). Transient inhibition of BMP signaling by Noggin induces cardiomyocyte differentiation of mouse embryonic stem cells. *Nat. Biotechnol.* **23**, 607-611.

Zaffran, S., Kelly, R. G., Meilhac, S. M., Buckingham, M. E. and Brown, N. A. (2004). Right ventricular myocardium derives from the anterior heart field. *Circ. Res.* **95**, 261-268.